ISSN: 2414-1895

DOI: 10.6919/ICJE.202510\_11(10).0009

# A MEMS Accelerometer that Utilizes Both Series and Differential Modes

Yuancheng Ouyang, Miao He\*
Guangdong University of Technology, Guangzhou, 510006, China

### **Abstract**

This paper presents an in-depth simulation analysis and optimized design of a MEMS accelerometer with a quadruple-cantilever structure, conducted using COMSOL Multiphysics. The simulation results reveal a fundamental mechanical characteristic: under acceleration load, the cantilever beam exhibits a strain distribution that is symmetric in magnitude but opposite in sign across its central axis (one side is under tensile strain while the other is under compressive strain). Leveraging this key insight, this study proposes an innovative series-parallel hybrid connection strategy. The four sensing elements on the two cantilevers are grouped according to their strain phases, enabling elements with identical strain to be connected in series for signal summation. The resultant anti-phase signals are then processed by a differential amplification circuit. This design successfully achieves two core advantages: firstly, through effective signal superposition and differential amplification, the final output signal amplitude is quadrupled compared to that of conventional single-ended accelerometers, significantly enhancing sensitivity. Secondly, the inherent common-mode rejection capability of the differential detection mechanism effectively suppresses environmental noise interference. This work provides a novel and effective solution for the design of highsensitivity and high-robustness MEMS accelerometers.

## **Keywords**

MEMS Accelerometer; COMSOL; Quadruple Output.

#### 1. Introduction

As a crucial type of inertial sensor, MEMS accelerometers have been widely adopted in several key fields. In consumer electronics, they are used for motion-sensing game controls and step detection in smart wearable devices [1]. In automotive electronics, they serve as core sensing elements for airbag deployment and electronic suspension systems [2]. In industrial automation, they are applied in robot balance control and structural health monitoring of large infrastructures [3]. Currently, MEMS accelerometers are primarily based on three sensing principles: capacitive, piezoresistive, and piezoelectric. Among these, piezoelectric accelerometers exhibit distinct advantages in specific applications such as impact monitoring, owing to their self-powering capability, wide measurement range, and long operational life [4-5]. However, compared to the extensively studied capacitive and piezoresistive types, research on piezoelectric accelerometers remains relatively limited. The performance of piezoelectric accelerometers is mainly determined by two key metrics: sensitivity and linearity. Sensitivity can be further broken down into: (1) signal conversion efficiency, which refers to the electrical signal output per unit acceleration input (typically expressed in pC/g or mV/g), and (2) resolution, which reflects the minimum detectable acceleration change and is closely related to the sensor's noise characteristics [6-9]. Regarding piezoelectric material selection, lead zirconate titanate (PZT), aluminum nitride (AlN), and zinc oxide (ZnO) are three commonly used materials. Compared to AlN and ZnO, PZT has become the preferred material for developing high-performance

ISSN: 2414-1895

DOI: 10.6919/ICJE.202510\_11(10).0009

MEMS piezoelectric accelerometers due to its superior piezoelectric properties [10-13]. Furthermore, among various thin-film deposition methods such as sol-gel, pulsed laser deposition (PLD), and MOCVD, magnetron sputtering offers significant advantages for depositing PZT films [14-17]. Firstly, the sputtering process takes place in a vacuum environment (typically at vacuum levels around 10<sup>-4</sup> Pa), effectively minimizing the incorporation of impurity gases and ensuring high film purity. Secondly, since the sputtering target has the same composition as the deposited film, precise control over the target composition and sputtering parameters enables highly consistent film stoichiometry, resulting in PZT films with excellent performance. Therefore, this paper adopts the magnetron sputtering method for PZT film preparation.

In recent years, researchers have conducted extensive studies on accelerometers based on PZT films. For example, in 2003, Wang Li-Peng et al. proposed a circular diaphragm accelerometer with four different silicon substrate thicknesses, achieving a charge sensitivity of 0.77-7.6~pC/g at the corresponding resonant frequencies <sup>[18]</sup>. In 2016, Bian Tian et al. developed an accelerometer with a specially shaped proof mass, achieving a sensitivity of 0.91~mV/g at 1279.1~Hz <sup>[19]</sup>. In 2021, Liyong Ma et al. fabricated a single-cantilever accelerometer with a sensitivity of 16.8~mV/g at an operating frequency of 200~Hz <sup>[20]</sup>. In 2022, Shuzheng Shi et al. designed an accelerometer with a centrally symmetric structure featuring four "L"-shaped cantilevers, reporting a maximum sensitivity of  $610~\pm~5~mV$  at the characteristic frequency of 815~Hz and a voltage sensitivity of 7.035~mV/g (charge sensitivity of 0.83~pC/g) at the reference operating frequency of 500~Hz <sup>[21]</sup>. In 2023, Xuewen Gong et al. developed a single-cantilever accelerometer designed for low-noise environments, achieving a sensitivity of up to 22.74~pC/g <sup>[22]</sup>. However, in these studies, the PZT film coverage on the cantilevers was relatively limited, preventing full utilization of the cantilever's potential.

This paper innovatively proposes and designs a novel MEMS piezoelectric accelerometer. The core innovation lies in a unique signal extraction and synthesis architecture: through a specific circuit connection design, the piezoelectric detection signals generated by two cantilever beams are synergistically integrated. This design fully utilizes the inherent, phase-complementary strain distribution characteristics of the cantilevers under stress, enabling the outputs of the two sensing elements to achieve effective superposition rather than simple algebraic addition. The results demonstrate that compared to traditional single-cantilever or independent signal processing schemes, the output signal amplitude of this accelerometer is significantly enhanced, thereby achieving an effective multiplication of sensitivity without altering the core mechanical structure dimensions. This work provides an effective technical pathway for breaking through the performance bottlenecks of MEMS piezoelectric sensors.

## 2. Operating Mode of PZT Thin Films Section Headings

To facilitate the analysis of the operating modes of PZT thin films, numerical indices can be used to define the direction of applied stress and the resulting electric field. First, the direction of stress and strain applied to the PZT film is defined as the 3-axis. The two mutually perpendicular axes in the plane normal to the 3-direction are defined as the 1-axis and 2-axis. For PZT thin films, only five piezoelectric coefficient components-d<sub>15</sub>, d<sub>24</sub>, d<sub>31</sub>, d<sub>32</sub>, and d<sub>33</sub>-are non-zero; all other components are zero. Furthermore, due to symmetry principles, the d<sub>31</sub> mode is effectively equivalent to the d<sub>32</sub> mode, and the d<sub>24</sub> mode is equivalent to the d<sub>33</sub> mode. Consequently, the primary operating modes of PZT thin films are the d<sub>31</sub>, d<sub>33</sub>, and d<sub>15</sub> modes [23]. Since the d<sub>15</sub> mode requires the PZT film to be subjected to shear stress-a condition difficult to achieve in practical applications-the most commonly utilized operating modes are the d<sub>31</sub> and d<sub>33</sub> modes.

The operating modes of the PZT thin film are illustrated in the fig. 1. According to the definition of the piezoelectric coefficient, the equation ( $D = d_{ij} \times S$ ) relates the strain S to the electric displacement D. In the  $d_{31}$  operating mode, the PZT thin film features planar electrodes. The polarization direction of the film is along the 1-axis, while it is subjected to strain along the 3-axis. Therefore, in this mode, when the PZT thin film experiences strain  $S_3$  along the 3-axis, it generates an electric displacement

ISSN: 2414-1895 DOI: 10.6919/ICJE.202510\_11(10).0009

D<sub>1</sub> along the 1-axis. In the d<sub>33</sub> operating mode, the PZT thin film utilizes interdigitated electrodes. The polarization direction is along the 3-axis, and the applied strain is also along the 3-axis. Consequently, in this mode, strain S<sub>3</sub> applied along the 3-axis produces an electric displacement D<sub>3</sub> along the 3-axis. Thus, in the d<sub>31</sub> and d<sub>33</sub> operating modes, the electric displacement generated by the PZT thin film is perpendicular and parallel to the direction of the applied strain, respectively.

Under normal conditions, the piezoelectric strain coefficient d<sub>33</sub> is 2–3 times greater than d<sub>31</sub> <sup>[24]</sup>. However, in the d<sub>31</sub> mode, parallel-plate electrodes (top and bottom electrodes) are used, which have a significantly larger area compared to the interdigitated electrodes employed in the d<sub>33</sub> mode. As a result, in terms of the total charge output, the d<sub>31</sub> mode yields a higher charge than the d<sub>33</sub> mode. Additionally, devices operating in the d<sub>33</sub> mode, due to the use of interdigitated electrodes with a smaller electrode area, exhibit a very high equivalent internal impedance. This leads to excessive energy dissipation within the device, thereby directly reducing the output power <sup>[25]</sup>. Therefore, the accelerometer developed in this study adopts the d<sub>31</sub> operating mode of the PZT thin film for signal harvesting. The principle is as follows: the inertial force of the central mass unit acts along the 3-axis of the PZT film on the cantilever beam, inducing a change in electric displacement-i.e., a variation in surface charge-on the upper and lower surfaces of the PZT film. The corresponding charge variation is given by:

$$Q=A \cdot S_3 \cdot d_{31} \tag{1}$$

where Q is the charge generated by the PZT thin film due to strain along the 3-axis, measured in coulombs (C); A represents the electrode area, measured in square meters ( $m^2$ );  $S_3$  denotes the strain along the 3-axis; and  $d_{31}$  is the piezoelectric coefficient, with units of coulombs per newton (C/N) or meters per volt (m/V).

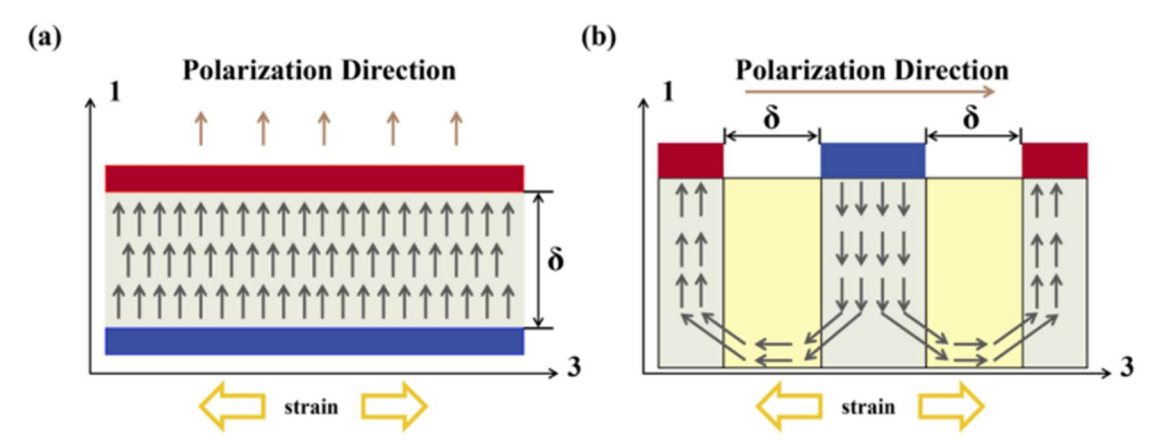


Fig. 1 PZT Thin Film Operating Modes: (a) d<sub>31</sub> Mode (b) d<sub>33</sub> Mode

## 3. Simulation and Design of Devices

In the design of piezoelectric MEMS accelerometers, cantilever beam structures demonstrate significant advantages due to their unique mechanical characteristics. The fixed-free configuration efficiently concentrates maximum strain near the fixed end under acceleration loads, leveraging the inertial effect of the proof mass at the free end, which has garnered considerable attention from researchers <sup>[26]</sup>. Moreover, cantilever structures exhibit excellent compatibility and reliability with mainstream MEMS processes: dry etching enables precise control of beam geometry, while sputter deposition facilitates the integration of piezoelectric/electrode multilayers. Additionally, the thickness of the cantilever can be effectively controlled by adjusting the device layer thickness of silicon-on-insulator (SOI) wafers. In this study, an in-depth simulation analysis of a four-cantilever MEMS accelerometer structure was conducted using COMSOL. The results indicate that when the

ISSN: 2414-1895 DOI: 10.6919

DOI: 10.6919/ICJE.202510\_11(10).0009

structure is subjected to external acceleration excitation, the root regions of the cantilevers become prominent stress concentration points. As shown in Fig. 2, the simulation not only reveals this stress concentration phenomenon but also clearly illustrates the symmetric deformation mode of the cantilevers: on either side of the geometric centerline, regions of the beam experience strains of equal magnitude but opposite signs. Combined with the previously explained working principle of the PZT thin film-where the generated charge is proportional to the applied strain-this behavior elucidates the operational mechanism of piezoelectric MEMS accelerometers.

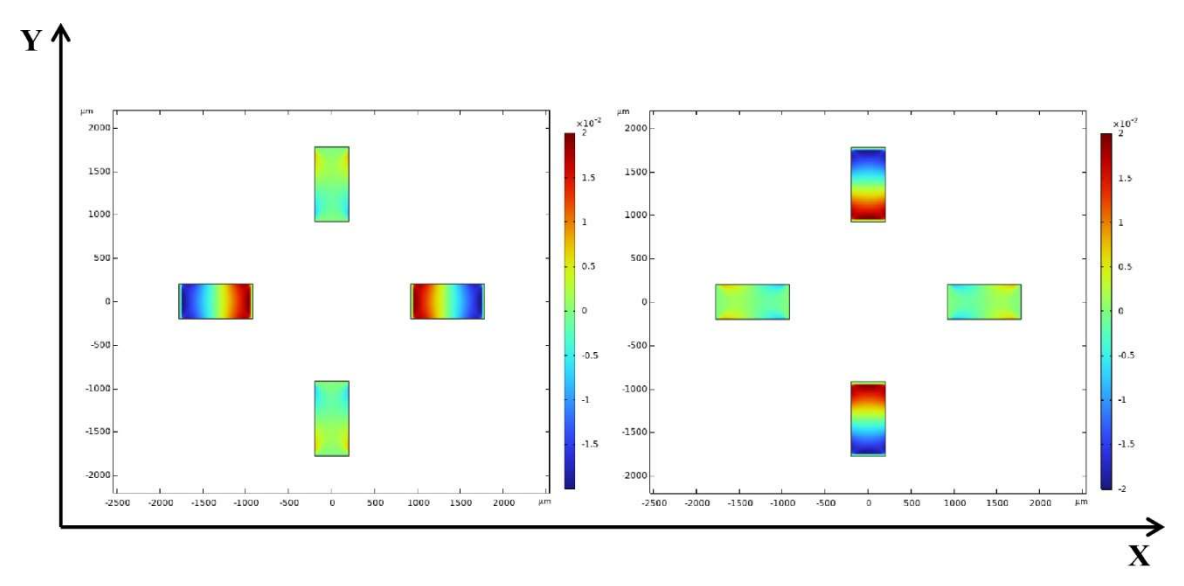


Fig. 2 Stress diagram of cantilever simulation

The operational schematic depicted in Fig. 3 illustrates this process: when the accelerometer experiences external acceleration, the proof mass generates an inertial force, causing the cantilever beam to undergo bending deformation. The resulting stress variation at the beam's root is precisely captured by the integrated PZT sensing thin film and converted into a corresponding electrical charge signal.

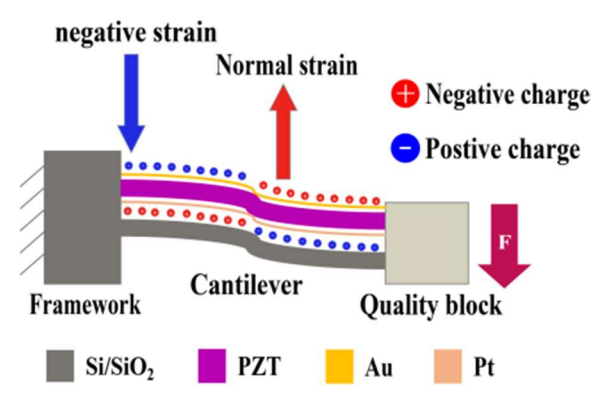


Fig. 3 Working principle of single cantilever

Based on the aforementioned conclusions, this study employs a configuration where sensing elements on different cantilevers are interconnected through both series and parallel connections. This design strategy effectively enhances the accelerometer's sensitivity while simultaneously suppressing common-mode noise and mitigating interference from external environmental factors such as temperature drift through the parallel connection scheme. The specific device implementation is illustrated in Fig. 4(left) below.

ISSN: 2414-1895 DOI: 10.6919/ICJE.202510\_11(10).0009

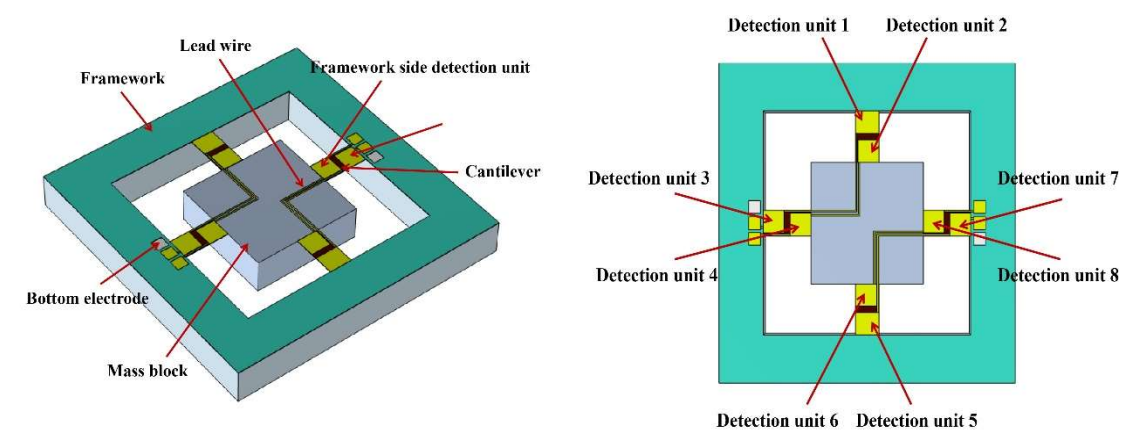


Fig. 4 Three-dimensional structural diagram of accelerometer

Based on COMSOL simulation results, under specific acceleration loading, the stress distribution of the sensing elements exhibits a clear pattern: elements 1, 3, 5, and 7 experience stresses of equal magnitude but opposite direction (phase), while elements 2, 4, 6, and 8 form another group with identical stress magnitude and opposite phase characteristics. Building on this phenomenon, our design strategy proceeds as follows: first, pairs of elements with opposite stress directions (specifically elements 1 & 3, 2 & 4, 5 & 7, and 6 & 8) are connected in series with reverse polarity, enabling their electrical signals to superimpose rather than cancel out. Subsequently, the resulting four series branches are connected in parallel to collectively output the total charge signal, thereby significantly enhancing both the sensitivity and signal-to-noise ratio of the sensor. This core design scheme is illustrated in Fig. 4 (right).

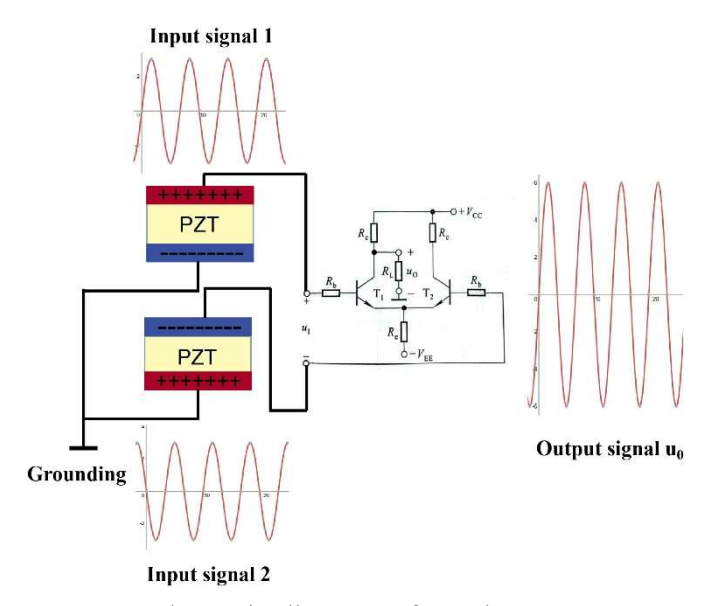


Fig. 5 Schematic diagram of accelerometer test

The signal detection scheme of this design is illustrated in Fig. 5. When the accelerometer is subjected to a sinusoidal acceleration excitation, the sensing elements on the cantilever beams generate charge signals with either identical phase or 180° phase difference. These signals with specific phase relationships are first fed into a differential amplifier, which not only effectively integrates signals from multiple channels but also suppresses common-mode noise, thereby outputting a waveform with significantly enhanced amplitude. Benefiting from the previously described series-parallel configuration, the electrical outputs from the four sensing elements are effectively superimposed. Both theoretical analysis and experimental results demonstrate that the final output signal amplitude

ISSN: 2414-1895

DOI: 10.6919/ICJE.202510\_11(10).0009

of this design can reach four times that of conventional single-element MEMS accelerometers, substantially improving detection sensitivity.

#### 4. Conclusion

This paper conducts an in-depth simulation analysis of the cantilever beam structure in a MEMS accelerometer using COMSOL Multiphysics software. The simulation results reveal a key mechanical distribution characteristic: under acceleration loading, the strain on the cantilever beam exhibits an antisymmetric distribution about its central axis. Specifically, the strain values in the left and right regions of the beam are equal in magnitude but opposite in sign (i.e., one side experiences tensile strain while the other experiences compressive strain). Building upon this inherent physical phenomenon, this study proposes an innovative design strategy: sensing elements located in regions with the same type of strain (e.g., all in tensile strain areas or all in compressive strain areas) on different cantilever beams are connected in series. This configuration ensures that their respective generated electrical signals (charge or voltage) undergo in-phase superposition. Subsequently, the combined signal is processed by a differential amplification circuit. This method synergistically achieves two core objectives: Firstly, by connecting four effective units in series, the output signal achieves a theoretical fourfold amplification compared to a single sensing element, significantly enhancing the device's sensitivity. Secondly, the inherent common-mode rejection capability of the differential amplifier effectively suppresses external interference signals such as power supply ripple and electromagnetic interference, thereby substantially improving the signal-to-noise ratio. Consequently, this work not only presents a high-performance accelerometer design scheme but also offers a novel and universally applicable design paradigm for the field of inertial sensing and motion detection.

## Acknowledgments

This work was supported by the Science and Technology Program of Zhongshan City, Guangdong Province [Grant Number 2023A4011].

#### References

- [1] Shanmugavel S, Yao K, Luong T D, et al. Miniaturized acceleration sensors with in-plane polarized piezoelectric thin films produced by micromachining[J]. IEEE transactions on ultrasonics, ferroelectrics, and frequency control, 2011, 58(11): 2289-2296.
- [2] Yazdi N, Ayazi F, Najafi K. Micromachined inertial sensors[J]. Proceedings of the IEEE, 2002, 86(8): 1640-1659.
- [3] Trifunovic M, Vadiraj A M, Van Driel W D. MEMS accelerometers and their bio-applications[C]//2012 13th International Thermal, Mechanical and Multi-Physics Simulation and Experiments in Microelectronics and Microsystems. IEEE, 2012: 1/7-7/7.
- [4] Tsai C C, Chien Y C, Hong C S, et al. Study of Pb (Zr0. 52Ti0. 48) O3 microelectromechanical system piezoelectric accelerometers for health monitoring of mechanical motors[J]. Journal of the American Ceramic Society, 2019, 102(7): 4056-4066.
- [5] Yang J, Zhang M, Si C, et al. A T-shape aluminum nitride thin-film piezoelectric MEMS resonant accelerometer[J]. Journal of Microelectromechanical Systems, 2019, 28(5): 776-781.
- [6] Krause A G, Winger M, Blasius T D, et al. A high-resolution microchip optomechanical accelerometer[J]. Nature Photonics, 2012, 6(11): 768-772.
- [7] Wu T, You D, Gao H, et al. Research status and development trend of piezoelectric accelerometer[J]. Crystals, 2023, 13(9): 1363.
- [8] Hewa-Kasakarage N N, Kim D, Kuntzman M L, et al. Micromachined piezoelectric accelerometers via epitaxial silicon cantilevers and bulk silicon proof masses[J]. Journal of microelectromechanical systems, 2013, 22(6): 1438-1446.
- [9] Kunz K, Enoksson P, Stemme G. Highly sensitive triaxial silicon accelerometer with integrated PZT thin film detectors[J]. Sensors and Actuators A: Physical, 2001, 92(1-3): 156-160.

DOI: 10.6919/ICJE.202510\_11(10).0009

- [10] Chen X, Qiao X, Zhang L, et al. Temperature dependence of ferroelectricity and domain switching behavior in Pb (Zr0· 3Ti0. 7) O3 ferroelectric thin films[J]. Ceramics International, 2019, 45(14): 18030-18036.
- [11] Yoshida S, Hanzawa H, Wasa K, et al. Highly c-axis-oriented monocrystalline Pb (Zr, Ti) O 3 thin films on si wafer prepared by fast cooling immediately after sputter deposition[J]. IEEE Transactions on Ultrasonics, Ferroelectrics, and Frequency Control, 2014, 61(9): 1552-1558.
- [12] Xu J, Zhang X, Fernando S N, et al. AlN-on-SOI platform-based micro-machined hydrophone[J]. Applied Physics Letters, 2016, 109(3).
- [13] Bhadwal N, Ben Mrad R, Behdinan K. Review of zinc oxide piezoelectric nanogenerators: piezoelectric properties, composite structures and power output[J]. Sensors, 2023, 23(8): 3859.
- [14] Suzuki H, Miwa Y, Naoe T, et al. Orientation control and electrical properties of PZT/LNO capacitor through chemical solution deposition[J]. Journal of the European Ceramic Society, 2006, 26(10-11): 1953-1956.
- [15] Wang J, Li Z, Zhang M, et al. High-quality ternary relaxor ferroelectric thin films on Si substrates by pulsed laser deposition method[J]. Journal of the American Ceramic Society, 2022, 105(6): 4089-4096.
- [16] Rice C E, Cuchiaro J D, Sun S, et al. Low temperature PZT film by MOCVD[J]. Integrated Ferroelectrics, 2003, 59(1): 1465-1473.
- [17] Ma Y, Song J, Wang X, et al. Synthesis, microstructure and properties of magnetron sputtered lead zirconate titanate (PZT) thin film coatings[J]. Coatings, 2021, 11(8): 944.
- [18] Wang L P, Wolf R A, Wang Y, et al. Design, fabrication, and measurement of high-sensitivity piezoelectric microelectromechanical systems accelerometers[J]. Journal of microelectromechanical systems, 2003, 12(4): 433-439.
- [19] Tian B, Liu H, Yang N, et al. Design of a piezoelectric accelerometer with high sensitivity and low transverse effect[J]. Sensors, 2016, 16(10): 1587.
- [20] Lee Y C, Tsai C C, Li C Y, et al. Fabrication and function examination of PZT-based MEMS accelerometers [J]. Ceramics International, 2021, 47(17): 24458-24465.
- [21] Shi S, Geng W, Bi K, et al. High sensitivity MEMS accelerometer using PZT-based four L-shaped beam structure[J]. IEEE Sensors Journal, 2022, 22(8): 7627-7636.
- [22] Gong X, Kuo Y C, Zhou G, et al. An aerosol deposition based MEMS piezoelectric accelerometer for low noise measurement[J]. Microsystems & Nanoengineering, 2023, 9(1): 23.
- [23] Wu Y, Ma Y, Zheng H, et al. Piezoelectric materials for flexible and wearable electronics: A review[J]. Materials & Design, 2021, 211: 110164.
- [24] Zhou W, Liao W H, Li W J. Analysis and design of a self-powered piezoelectric microaccelerometer[C]//Smart Structures and Materials 2005: Smart Electronics, MEMS, BioMEMS, and Nanotechnology. SPIE, 2005, 5763: 233-240.
- [25] Wen J H, Fang W. Novel pure-metal tri-axis CMOS-MEMS accelerometer design and implementation[J]. Micro & Nano Letters, 2021, 16(12): 567-572.
- [26] Hao M, Chen A J. Drop\*\* impact characteristics analysis of a cubic nonlinear packaging system with a cantilever beam type elastic critical component with concentrated tip mass[J]. Shock and Vibration, 2015, 2015(1): 602984.